

1995120929

405363  
N95-27350

## VALIDATION OF THE SINDA/FLUINT CODE USING SEVERAL ANALYTICAL SOLUTIONS

John R. Keller  
Lockheed Engineering and Sciences Company  
Houston, Texas

35-34  
45098  
p-16

### ABSTRACT

The Systems Improved Numerical Differencing Analyzer and Fluid Integrator (SINDA/FLUINT) code has often been used to determine the transient and steady-state response of various thermal and fluid flow networks. While this code is an often used design and analysis tool, the validation of this program has been limited to a few simple studies.

For the current study, the SINDA/FLUINT code was compared to four different analytical solutions. The thermal analyzer portion of the code (conduction and radiative heat transfer, SINDA portion) was first compared to two separate solutions. The first comparison examined a semi-infinite slab with a periodic surface temperature boundary condition. Next, a small, uniform temperature object (lumped capacitance) was allowed to radiate to a fixed temperature sink. The fluid portion of the code (FLUINT) was also compared to two different analytical solutions. The first study examined a tank filling process by an ideal gas in which there is both control volume work and heat transfer. The final comparison considered the flow in a pipe joining two infinite reservoirs of pressure. The results of all these studies showed that for the situations examined here, the SINDA/FLUINT code was able to match the results of the analytical solutions.

### INTRODUCTION

The Systems Improved Numerical Differencing Analyzer and Fluid Integrator (SINDA/FLUINT) program has often been used to determine the transient hydrodynamic and thermal response of various thermal and fluid networks. For example, the Space Station Freedom's (SSF) Active Thermal Control System (ATCS) [1] and airlock [2], the Space Shuttle's ATCS [3], and the SSF's Lunar Transport Vehicle Hangar [4] have all been analyzed using this code. While this code has provided important results in the design and analysis of these and other space related hardware, the validation of this program has been limited.

The validation of any numerical code is important, since once a code has been verified for several test cases, a user will have confidence that the code can accurately predict the physical processes of other, more complex problems. In general, there are three main verification methods. The first method compares the predicted results with those of a previously validated code [5]. The second method uses experimental data to verify the model's predictions [6]. Finally, the predicted results can be compared to those of a closed form analytical solution [7].

To date, the SINDA/FLUINT code has been validated with three simple closed form solutions [8,9,10] and one relatively complex experimental comparison [11]. The three closed form solutions considered were the transient conduction in a semi-infinite slab [8], the filling and decompression of a rigid, adiabatic tank with an ideal gas [9], and the transient heat transfer associated with a single phase fluid flowing in a duct [10]. The experimental comparison examined the combined radiative, conductive, and convective heat rejection process associated with the operation of the Space Shuttle's ATCS during orbital conditions [11]. For all the tests cases considered, the predictions of the SINDA/FLUINT code were able to match the results of either the closed form solutions or the experimental data; however, the program has yet to be validated for more complex situations such as transient radiation, conduction or fluid flow phenomenon.

This paper details a validation study of the SINDA/FLUINT program for several simple situations. The code was validated by comparing its results with those of several closed form analytical solutions. The SINDA portion of the code was compared to two different analytical solutions, while the FLUINT portion of the code was also validated with two separate analytical solutions. The results of these studies showed that for the situations examined here, the code was able to accurately predict the heat transfer and fluid flow processes.

## HEAT TRANSFER IN A SEMI-INFINITE SOLID

The SINDA portion of the code was first validated using the classical closed form solution for conduction heat transfer in a semi-infinite solid. For this test case, a periodic surface temperature boundary condition was considered. A schematic of this system and its associated boundary condition is shown in Figure 1.

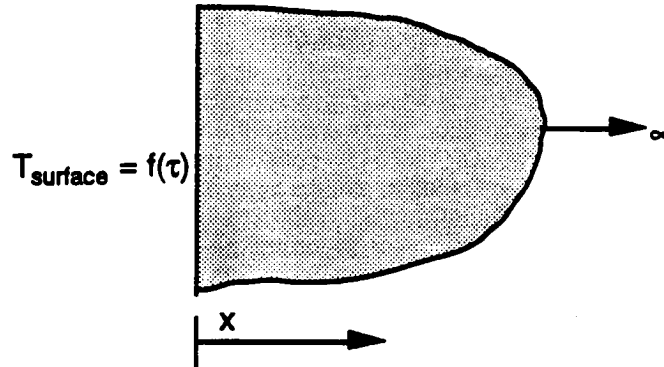


Figure 1 Schematic of a Semi-Infinite Solid.

The heat conduction in a semi-infinite solid, with no internal generation and constant thermophysical properties, is governed by the following differential equation,

$$\frac{\partial^2 T}{\partial x^2} = \frac{1}{\alpha} \frac{\partial T}{\partial \tau} \quad (1)$$

where the variables  $T$ ,  $x$ ,  $\alpha$ , and  $\tau$  are the temperature, distance, thermal diffusivity, and time, respectively. To reduce the complexity of the solution process, the temperature is replaced by a new variable,  $\Theta$ , which is defined as

$$\Theta = T - T_i \quad (2)$$

where the subscript  $i$  denotes the initial condition. The new governing equation and the boundary conditions for this problem are

$$\frac{\partial^2 \Theta}{\partial x^2} = \frac{1}{\alpha} \frac{\partial \Theta}{\partial \tau} \quad (3)$$

$$\Theta(x, 0) = 0 \quad (4)$$

$$\Theta(\infty, \tau) = 0 \quad (5)$$

$$\Theta(0, \tau) = \Theta_0 \cos \omega \tau \quad (6)$$

where  $\Theta_0$  and  $\omega$  are the amplitude and frequency, respectively. To obtain a solution for equation (3), the separation of variables method must be used and for brevity will not be presented here. A detailed discussion of this solution procedure can be found in Reference 12. The solution to equation (3) with the appropriate boundary conditions is

$$\frac{\Theta(x, t)}{\Theta_0} = e^{-(\omega/2\alpha)^{1/2} x} \cos \left[ \omega \tau - \left( \frac{\omega}{2\alpha} \right)^{1/2} x \right] \quad (7)$$

It is important to note that equation (7) is only valid for large values of time since there is a discontinuity at the initial conditions. In other words, equation (7) cannot accurately predict transient effects during the first increase of the solid's outer surface.

Once the analytical solution had been obtained for conduction in a semi-infinite solid, a SINDA model was built for the comparison study. A schematic of this SINDA model is shown in Figure 2. Here, a series of nodes with a height and depth of unity are placed together. The lengthwise spacing and thermophysical properties are input parameters and chosen in such a way that the computational process is simplified.

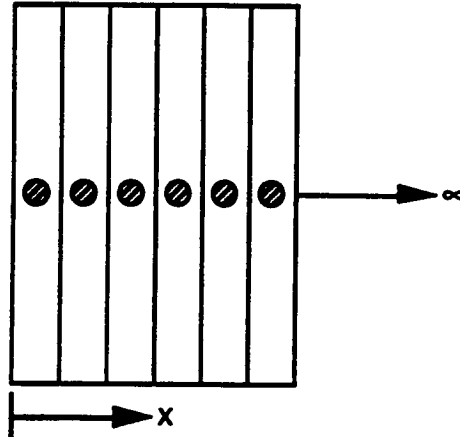


Figure 2 Schematic of the SINDA model.

Figure 3 shows the comparison between the results of the SINDA model and those of the analytical solution at different depths into the semi-infinite slab. As anticipated, the predictions show an exponential decay in the oscillating temperature as the depth into the solid increases. In addition, the predictions also show a phase shift in the oscillating temperatures and is associated with the time it takes the heat to be conducted into the solid. As is evident, for the parameters examined here, the predictions are nearly identical to those of the analytical solution. The greatest temperature difference between the results of the two solutions is less than 1.25 °F. Other conditions were also examined and a similar error was noted.

## COOLING BY RADIATIVE HEAT TRANSFER

The SINDA portion of the code was next validated using a closed form solution of a simple radiative cooling process in which a warm object cools by thermal radiation to a cold sink. To simplify the analysis, the lumped capacitance method was employed and the object radiated to one source. In other words, the entire solid was at a uniform temperature, one cold sink was available and there was no reflected radiation. To further simplify the analysis, the radiating source was taken to be diffusive. Applying these assumptions, the heat loss,  $Q$ , at an instant in time is given by

$$Q = \epsilon A \sigma [T^4 - T_{\text{sink}}^4] \quad (8)$$

where  $\epsilon$  is the emissivity,  $A$  is the surface area,  $\sigma$  is the Stefan-Boltzmann constant,  $T$  is the object's lumped temperature, and  $T_{\text{sink}}$  is the radiative sink temperature. Rewriting equation (8) for transient conditions and using the lumped capacitance assumption yields

$$-\rho V C_p \frac{\partial T}{\partial \tau} = Q = \epsilon A \sigma [T^4 - T_{\text{sink}}^4] \quad (9)$$

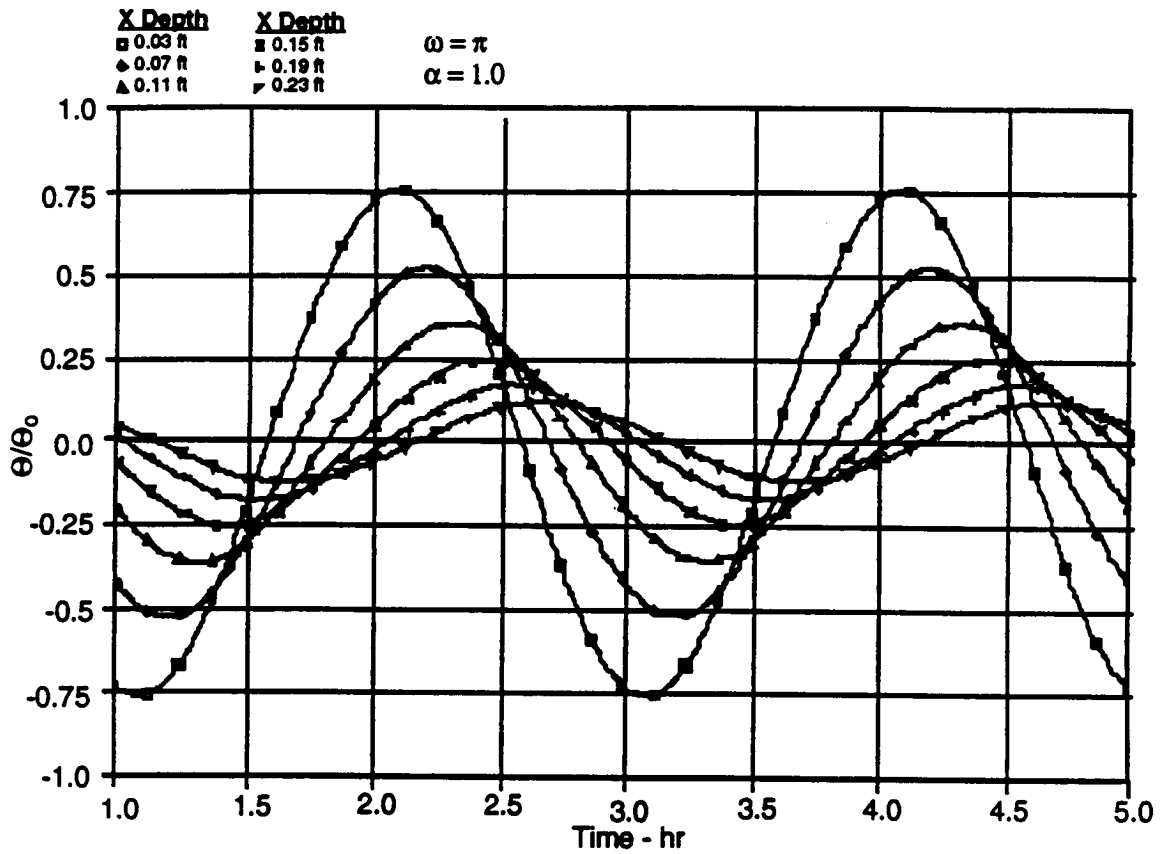


Figure 3 Temperature Response for Predicted (geometric shapes) and Analytical Solutions (solid lines).

where the new variables  $\rho$ ,  $V$ ,  $C_p$ , and  $\tau$  represent the density, volume, the specific heat and time, respectively. Rearranging and integrating equation (9) yields,

$$\int_{T=T_i}^{T=T_f} \frac{\partial T}{T^4 - T_{\text{sink}}^4} = \frac{\epsilon A \sigma}{\rho V C_p} \int_0^{\tau} \partial \tau \quad (10)$$

where  $T_i$  and  $T_f$  are the initial and final temperatures, respectively. Carrying out the integration on equation (10), yields equation (11)

$$\tau = \frac{\rho V C_p}{\epsilon A \sigma} \left[ \frac{1}{4T_{\text{sink}}^3} \ln \left( \frac{(T_f + T_{\text{sink}})/(T_f - T_{\text{sink}})}{(T_i + T_{\text{sink}})/(T_i - T_{\text{sink}})} \right) + \frac{1}{2T_{\text{sink}}^3} \left( \tan^{-1} \frac{T_f}{T_{\text{sink}}} - \tan^{-1} \frac{T_i}{T_{\text{sink}}} \right) \right] \quad (11)$$

Equation (11) reveals that for a given initial temperature, the final temperature is governed by the time,  $\tau$ , the sink temperature,  $T_{\text{sink}}$ , and the term,  $\rho V C_p / \epsilon A \sigma$ , (capacitance divided by radiative conductance). These terms were varied during the verification process. For the present study, the sink temperature was held at either -100 °F, -200 °F or -400 °F, while the capacitance-conductance ratio was set at 0.25, 0.5, 1.0 and 4.0. For each simulation, the initial temperature was held at 70 °F and the object was allowed to cool for 10 hours.

The results from both the SINDA model and the analytical solution for all the above conditions are shown in Figure 4. As expected, the cooling process follows a typical exponential decay, and the higher capacitance (or lower radiative conductance) objects cool more slowly. As is evident, the SINDA generated results are in good agreement with those of the analytical solution, since the predicted results are nearly identical to those of the analytical solution. The greatest temperature difference between the results of the two solutions is less than 1.5 °F, which corresponds to an error based on absolute temperature of less than 0.5% .

## FLOW BETWEEN TWO INFINITE RESERVOIRS OF PRESSURE

When two infinite reservoirs of different pressure are connected by a circular duct, such as those shown in Figure 5, the flow rate between the two, neglecting any entrance effects, is related by the following expression,

$$\Delta P = \rho f \frac{L}{D} \frac{V^2}{2} \quad (12)$$

where  $P$  is the pressure,  $\rho$  is the density of the working fluid,  $f$  is the friction factor,  $L$  is the length of the duct,  $D$  is the diameter of the duct, and  $V$  is the velocity of the fluid.

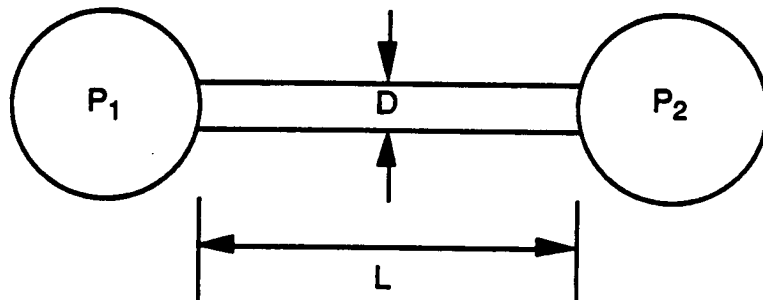


Figure 5 Schematic of the System.

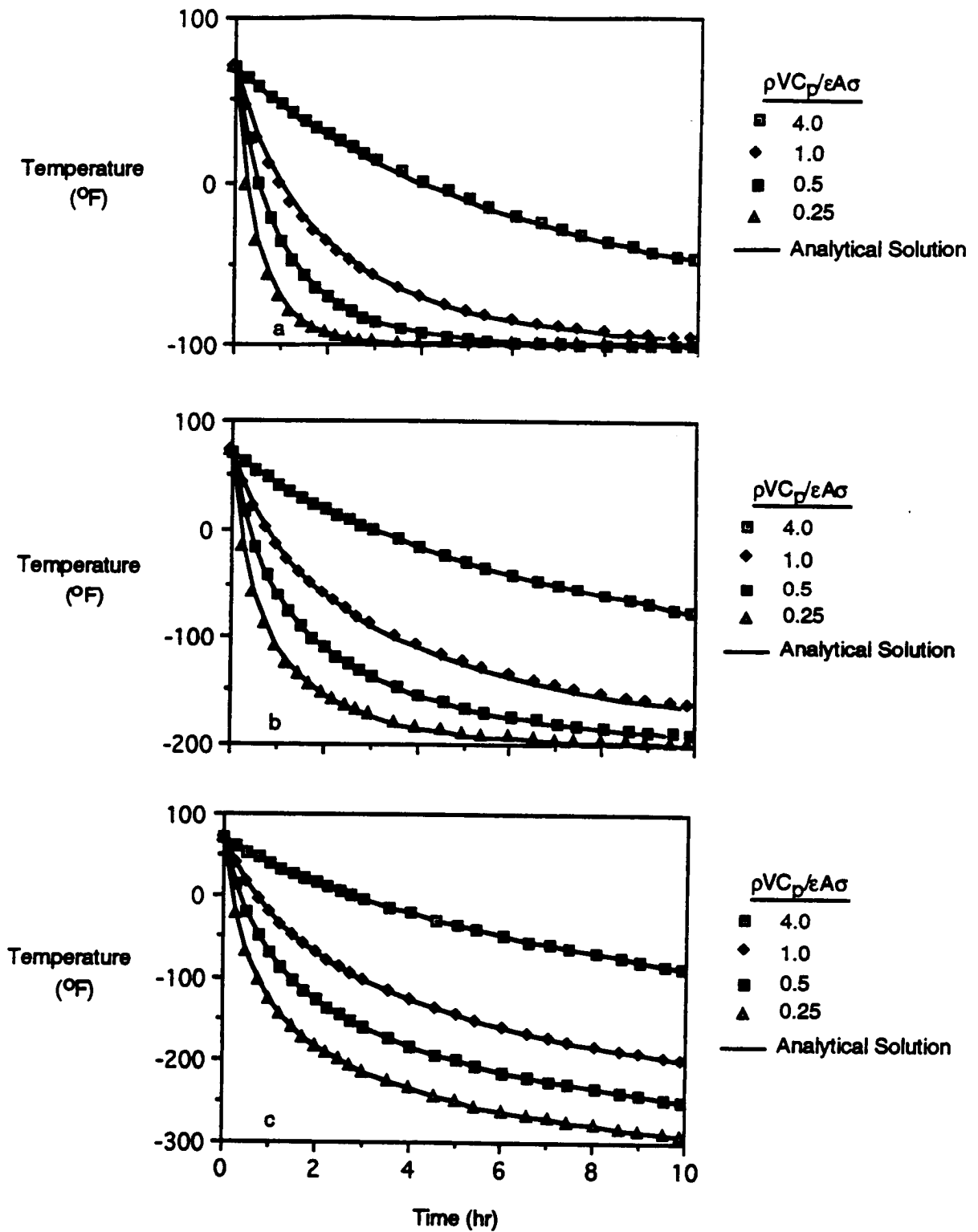


Figure 4 Predicted Temperature Response for Various Capacitance-Conductance Ratios for a)  $T_{\text{sink}} = -100^\circ\text{F}$ , b)  $T_{\text{sink}} = -200^\circ\text{F}$ , and c)  $T_{\text{sink}} = -400^\circ\text{F}$ .

The velocity of the fluid is related to the mass flow rate by

$$V = m/\rho A \quad (13)$$

where  $m$  is the mass flow rate and  $A$  is the cross sectional area of the duct. The area of the duct is given by

$$A = \pi D^2/4 \quad (14)$$

Substituting equations (13) and (14) into equation (12) and rearranging yields

$$\Delta P = \frac{8fm^2L}{\rho\pi^2D^5} \quad (15)$$

Solving for the friction factor gives

$$f = \frac{\Delta P \rho \pi^2 D^5}{8m^2 L} \quad (16)$$

For laminar flow the friction factor is given by

$$f = 64/Re \quad (17)$$

where  $Re$  is the Reynolds number which is given by

$$Re = \frac{VD}{\nu} \quad (18)$$

where  $\nu$  is the kinematic viscosity. For turbulent flow the friction factor is a function of the Reynolds number and the wall roughness ratio ( $e/D$ ). The value of turbulent friction factors must be determined experimentally and can be found on the Moody chart [13]. Reviewing equations (12) through (16) shows that for a given fluid if the pressure difference, pipe diameter and length are fixed, the velocity can be determined, directly for laminar flow and iteratively for turbulent flow. As such, any numerical code that is developed correctly should be able to accurately predict fluid velocities when the other parameters are fixed.

For the system shown in Figure 5, a simple FLUENT model was developed. The duct was represented by the TUBE option so that internal pipe friction would be included in the model. The pressure source and sink were represented by plenums (PLEN in FLUENT) which maintained a constant pressure at the ends of the TUBE. A schematic of this FLUENT model is shown in Figure 6.

For the current study, the pressures of the PLENS, and the pipe length and diameter of the TUBE are fixed. The model is then run in a steady-state mode until a converged solution is obtained. Using this flow rate, the friction factor and Reynolds number were calculated (Equation (16) and (18)) and compared to the analytical solutions. If the FLUENT code is properly developed, the predictions should match the analytical solution or the Moody chart values.

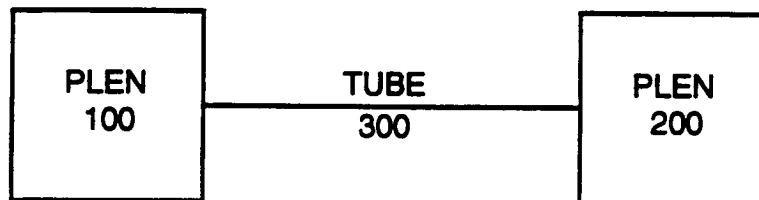


Figure 6 Schematic of the FLUENT Model.

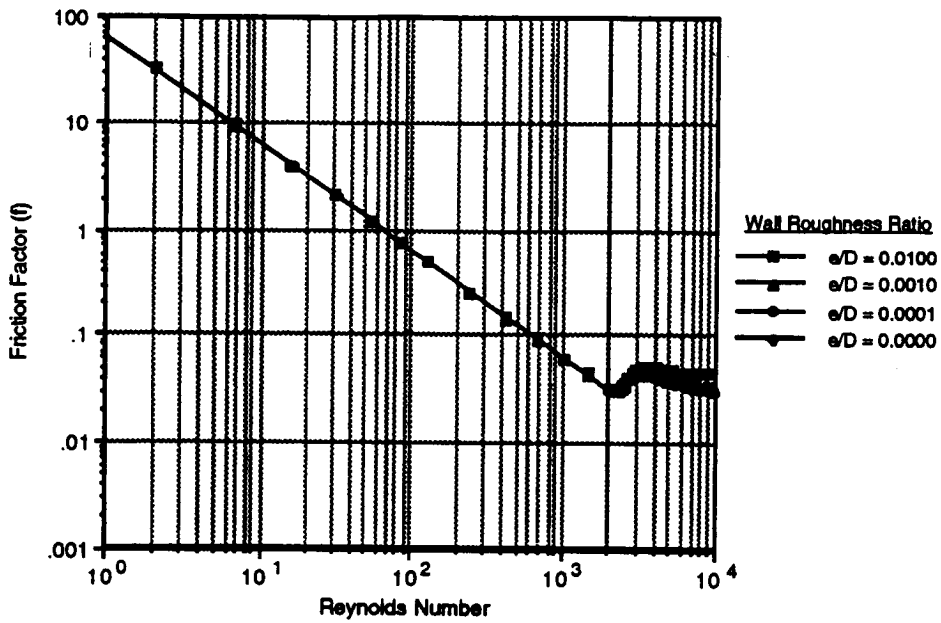


Figure 7 Predicted and Actual (Solid Line —) Reynolds Number in the Laminar Region for Various Wall Roughness Ratios.

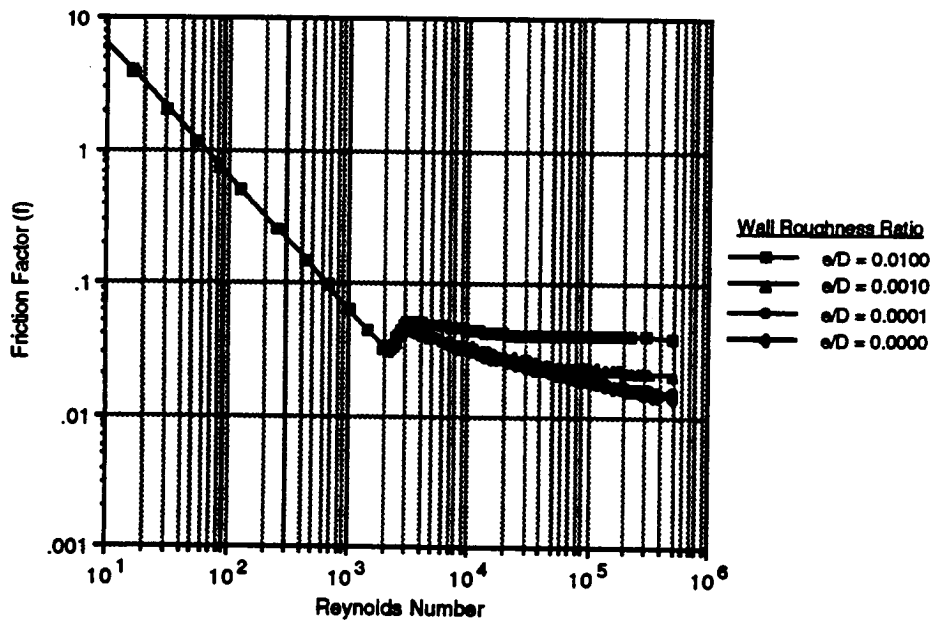


Figure 8 Predicted and Actual (Solid Line —) Reynolds Number in the Turbulent Region for Various Wall Roughness Ratios.



The model was run over Reynolds numbers ranging from 1 to  $10^6$  for four different values of  $e/D$  and the predicted friction factors can be found in Figures 7 and 8. When laminar flow was considered (Figure 7), the friction factor was found to be independent of the wall roughness and a linear function of the Reynolds number. For this situation, the predicted FLUENT results are nearly identical ( $< 0.1\%$ ) to those of the analytical solution.

When the flow is turbulent ( $Re > 2300$ ), the friction in the pipe is a function of the both the Reynolds number and the wall roughness. The greater the wall roughness, the greater the friction factor. The predicted friction factors in the turbulent regime for various wall roughness ratios can be found in Figure 8. As is evident, the predicted friction factors agree with those taken from the Moody chart and also shows the dependence of the friction factor upon wall roughness after the laminar regime.

## TANK FILLING WITH HEAT TRANSFER AND CONTROL VOLUME WORK

### Development of the Analytical Solution

Many thermodynamic processes involve unsteady flow and are difficult to analyze; however, several processes, such as the filling of a closed container, can be approximated by a simplified model. These types of problems are known as uniform-state, uniform-flow (USUF) processes. The basic assumptions for this flow condition are as follows:

- 1) The thermodynamic state of the mass within the control volume may change with time, but at any instant of time the state is uniform throughout the entire control volume.
- 2) The thermodynamic state of the mass entering the control volume is constant with time.

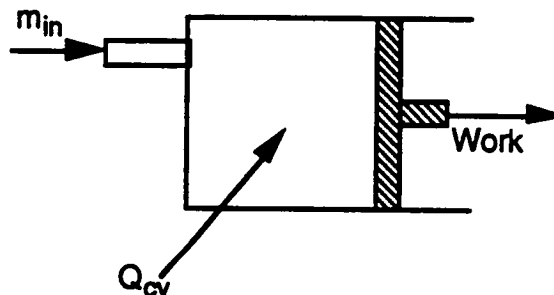


Figure 9 Schematic of the System.

Using these assumptions and Figure 9 as a guide, the first law [14] can be simplified for a tank filling scenario with heat transfer and control volume work. With no velocity or gravity potential terms, the first law for this tank filling process is,

$$m_2 h_2 = m_1 h_1 + W_{cv} + Q_{cv} \quad (19)$$

where  $m$  is the mass,  $h$  is the enthalpy,  $u$  is the internal energy,  $W_{cv}$  is the total control volume work, and  $Q_{cv}$  is the total heat transfer. The subscripts in, 2, and 1 denote the inlet, final and initial states, respectively. From the continuity equation, the following relationship can also be developed.

$$m_2 = m_1 + m_{in} \quad (20)$$

Substituting equation (20) into equation (19), replacing the enthalpy with  $C_p T$  and the internal energy with  $C_v T$  (the assumption of constant specific heats) yields

$$(m_2 - m_1)C_p T_{in} = m_2 C_v T_2 - m_1 C_v T_1 + W_{cv} + Q_{cv} \quad (21)$$

where  $C_p$ ,  $C_v$  and  $T$  are the constant pressure specific heat, the constant volume specific heat and temperature, respectively. Incorporating the ideal gas law ( $PV=RT$ ) into equation (21) gives

$$\left(\frac{P_2 V_2}{RT_2} - \frac{P_1 V_1}{RT_1}\right) C_p T_{in} = \frac{P_2 V_2}{RT_2} C_v T_2 - \frac{P_1 V_1}{RT_1} C_v T_1 + W_{cv} + Q_{cv} \quad (22)$$

where  $P$  is the pressure,  $V$  is the volume, and  $R$  is the specific gas constant. Rearranging equation (22) produces

$$\left(\frac{P_2}{T_2} - \frac{P_1 V_1}{T_1 V_2}\right) C_p T_{in} = \left(P_2 - \frac{P_1 V_1}{V_2}\right) C_v + \frac{W_{cv} R}{V_2} + \frac{Q_{cv} R}{V_2} \quad (23)$$

Dividing by the constant volume specific heat,  $C_v$ , and defining a new variable

$$\frac{V_1}{V_2} = \frac{1}{V_r} \quad (24)$$

equation (5) becomes,

$$\left(\frac{P_2}{T_2} - \frac{P_1}{T_1 V_r}\right) k T_{in} = \left(P_2 - \frac{P_1}{V_r}\right) + \frac{W_{cv} R}{C_v V_2} + \frac{Q_{cv} R}{C_v V_2} \quad (25)$$

where  $k$  is the ratio of the specific heats. Rearranging equation (7) gives

$$\frac{P_2}{T_2} = \frac{P_2 V_r - P_1}{k T_{in} V_r} + \frac{P_1}{T_1 V_r} + \frac{W_{cv} R}{k T_{in} C_v V_2} + \frac{Q_{cv} R}{k T_{in} C_v V_2} \quad (26)$$

Solving for the final temperature gives,

$$T_2 = \frac{P_2}{\left(\frac{P_2 V_r - P_1}{k T_{in} V_r} + \frac{P_1}{T_1 V_r} + \frac{W_{cv} R}{k T_{in} C_v V_2} + \frac{Q_{cv} R}{k T_{in} C_v V_2}\right)} \quad (27)$$

Further simplification yields,

$$T_2 = \frac{k P_2 T_1 T_{in} V_r}{\left((P_2 V_r - P_1) T_1 + k P_1 T_{in} + \frac{W_{cv} R T_1}{C_v V_1} + \frac{Q_{cv} R T_1}{C_v V_2}\right)} \quad (28)$$

Reviewing equation (28) shows that when work or heat leaves the control volume, the final temperature will be reduced compared to a system in which these quantities are absent. It is also important to note that in the absence of work and heat transfer, equation (28) reduces to a common equation that is used to estimate final temperatures in rigid adiabatic containers [14].

In writing equation (28) it is assumed that the total work,  $W_{cv}$ , that occurs between the initial (1) and final (2) states is known or can be determined. In general, the work term is not constant and varies with both system pressure and volume. From thermodynamic relationships [14], the total control volume work is defined as

$$W_{cv} = \int_1^2 P dV \quad (29)$$

Typically, volume is related to the pressure by an arbitrary function.

$$V = f(P) \quad (30)$$

Similarly the pressure is related to the volume by the inverse function

$$P = f^{-1}(V) \quad (31)$$

Replacing the pressure term in equation (29) with equation (31) gives

$$W_{cv} = \int_1^2 f^{-1}(V) dV \quad (32)$$

For the present study, the function,  $f(P)$ , was chosen so that the integral could easily be evaluated. The manipulation of the SINDA/FLUINT code to include control volume work will be discussed shortly in an upcoming section.

### Development of the SINDA Model

Figure 10 shows a schematic of the FLUINT model that was used to validate the code. Here, a TANK is connected to a PLEN (PLEN<sub>um</sub>) by an MFRSET (Mass Flow Rate SET). By using the TANK option, the first assumption for USUF processes (uniform state within the control volume) is met. The use of the PLEN ensures that the second USUF assumption of constant inlet properties is also maintained. To ensure that the working fluid is an ideal gas, an 8000 series fluid, using nitrogen as the working fluid, was developed and employed.

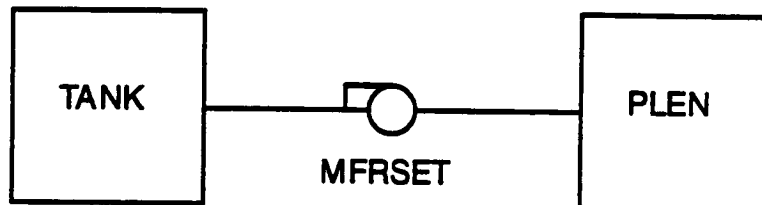


Figure 10 Schematic of the FLUINT Model.

While the SINDA/FLUINT program does not directly calculate (include) work terms for expanding (or contracting) control volumes, the code does calculate the thermal and hydraulic response of compliant (soft) TANKs. In the code, the compliance is defined as

$$COMP = \frac{1}{V} \frac{dV}{dP} \quad (33)$$

Therefore, if there is a function relating pressure and volume, an expanding control volume can be included in the FLUINT model, and by using equations (29) through (32), the control volume work can then be determined for the analytical solution.

Before the results are examined, it is important to first review the analytical solution. Equation (28) has been derived from a basic thermodynamic equation which was integrated over time. While the FLUINT code uses a rate based thermodynamic equation, the code integrates this equation over small discretized time intervals and the starting conditions at one time step are taken from the final conditions of the previous time step. This procedure employed by the FLUINT is the numerical equivalent of an integration. Since FLUINT has been developed using rate based

equations and the analytical solution uses overall heat transfer, one of the solution methods must be modified. To modify the heat transfer terms so that they can be included in the analytical solution, all that is required is that the FLUINT heat transfer term (QDOT in FLUINT) be multiplied by the total run time (TIMEN) and thus total heat transfer.

## Results

The comparison study was conducted in several steps. First, the model considered situations where only heat transfer or the volume changed. The model was then run for situations in which there was both simultaneous heat transfer and control volume work. For all the cases examined, the initial pressure and temperature within the storage container was set to 100 psia and 70 °F, respectively, while the inlet temperature was held to 70 °F. The final pressure of the tank was limited to 1000 psia. The volume of the TANK was initially set to 0.5 ft<sup>3</sup>. The results from these studies are summarized in Tables 1 through 4.

Figure 11 shows the predicted control volume temperature as a function of pressure for a variety of cooling rates with a fixed volume. As expected, the greater the heat loss, the lower the predicted temperature. In other words, a portion of the heat of compression is removed, resulting in lower predicted temperatures. More importantly, however, is to note that regardless of the heat transfer rate, the predictions are nearly identical to those of the analytical solution.

Figure 12 presents the analytical and predicted control volume temperature as a function of pressure for various heating rates. For these cases, the higher the heat addition, the higher the final volume temperature. Again, the predicted results are nearly identical to those of the analytical solution.

Figure 13 shows the predicted and analytical solution temperatures for the situation of an expandable control volume in which there is no heat transfer. Since a portion of the working fluid's energy must be used to produce work, the temperatures are lower than for the case in which the volume is fixed. For this situation too, the code was able to predict results nearly identical to those of the analytical solution.

Figure 14 presents the analytical and predicted temperatures for the conditions which include both control volume work and heat transfer. The volume is equal to the pressure multiplied by a constant. Depending on the situation examined, the predicted temperature was either greater (heating) or less (cooling) than the base case. As is evident, the code was able to match the results of the analytical solution.

## SUMMARY AND CONCLUSIONS

This paper details a validation study of the SINDA/FLUINT program for several simple situations and focused on the major building blocks of the SINDA and FLUINT portions of the code. The code was validated by comparing its results with those of four closed form solutions. The thermal analyzer portion of the code (conduction and radiative heat transfer, SINDA portion) was first compared to two separate solutions. The first comparison examined a semi-infinite slab with a periodic surface temperature boundary condition. Next, a small, uniform temperature object (lumped capacitance) was allowed to radiate to a fixed temperature sink. The fluid portion of the code (FLUINT) was also compared to two different analytical solutions. The first study examined a tank filling process by an ideal gas in which there is both control volume work and heat transfer. The final comparison considered the flow in a pipe joining two infinite reservoirs of pressure. The results of all these studies showed that for the situations examined here, the SINDA/FLUINT code was able to match the results of the analytical solutions.

To date only one large scale SINDA/FLUINT model has been built and used to validate the FLUINT code [11] and the interaction between SINDA/FLUINT modeling components has yet to be examined. Therefore, future studies should be devoted to building large sized models which can be verified by either analytical solutions or experimental data.

**Table 1** Predicted and Analytical Temperatures for Various Heat Loading Conditions.  
Initial Conditions  $P_1 = 100$  psia,  $T_1 = 70$  °F,  $T_{in} = 70$  °F,  $P_{final} = 1000$  psia

SINDA/FLUINT $T_{final}$ (°F)	Analytical $T_{final}$ (°F)	Q (Btu/hr)	Volume Relationship
253.02	253.46	0.0	V=C
241.29	241.63	-500.0	V=C
229.58	229.75	-1000.0	V=C
193.65	193.64	-2500.0	V=C
132.69	132.30	-5000.0	V=C
5.77	5.05	-10000.0	V=C

**Table 2** Predicted and Analytical Temperatures for Various Heat Loading Conditions.  
Initial Conditions  $P_1 = 100$  psia,  $T_1 = 70$  °F,  $T_{in} = 70$  °F,  $P_{final} = 1000$  psia

SINDA/FLUINT $T_{final}$ (°F)	Analytical $T_{final}$ (°F)	Q (Btu/hr)	Volume Relationship
253.02	253.46	0.0	V=C
264.57	265.22	500.0	V=C
276.13	276.96	1000.0	V=C
310.59	311.76	2500.0	V=C
366.44	368.39	5000.0	V=C
473.25	476.80	10000.0	V=C

**Table 3** Predicted and Analytical Temperatures for Volume Relationships  
Initial Conditions  $P_1 = 100$  psia,  $T_1 = 70$  °F,  $T_{in} = 70$  °F,  $P_{final} = 1000$  psia

SINDA/FLUINT $T_{final}$ (°F)	Analytical $T_{final}$ (°F)	Q (Btu/hr)	Volume Relationship
253.02	253.46	0.0	V=C
156.12	157.01	0.0	V=CP
125.55	125.38	0.0	V=CP <sup>2</sup>
189.30	189.66	0.0	V=CP <sup>1/2</sup>

**Table 4** Predicted and Analytical Temperatures for Various Heat Loading Conditions and  
Volume Relationships.  
Initial Conditions  $P_1 = 100$  psia,  $T_1 = 70$  °F,  $T_{in} = 70$  °F,  $P_{final} = 1000$  psia

SINDA/FLUINT $T_{final}$ (°F)	Analytical $T_{final}$ (°F)	Q (Btu/hr)	Volume Relationship
156.12	157.01	0.0	V=CP
133.83	133.70	-1000.0	V=CP
180.19	180.29	1000.0	V=CP
40.84	40.21	-5000.0	V=CP
272.59	273.57	5000.0	V=CP

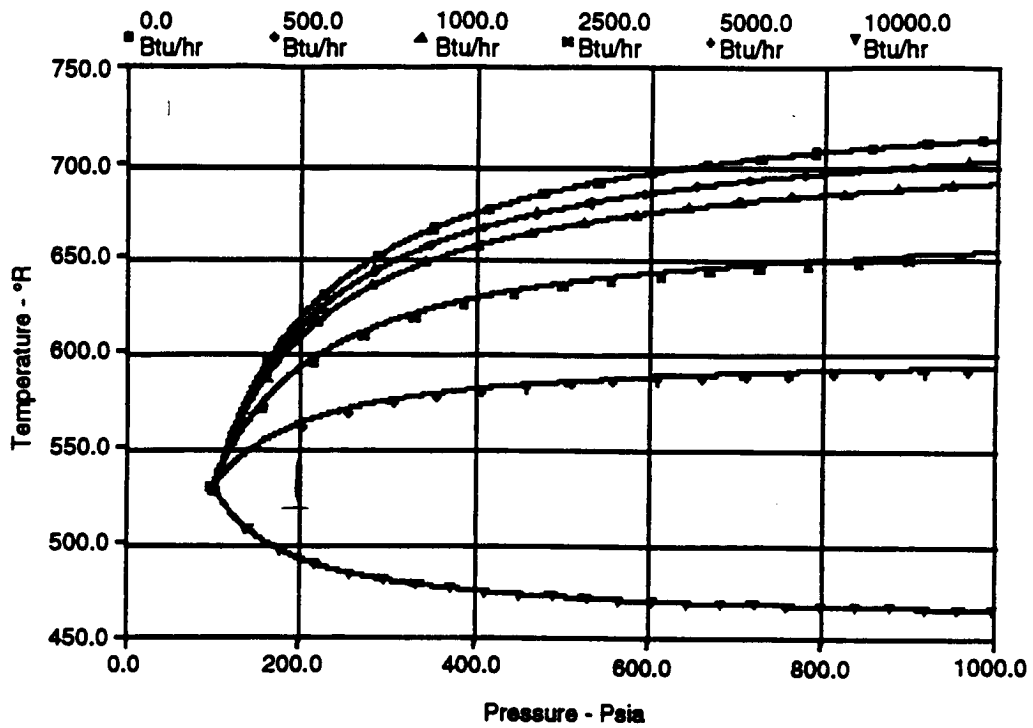


Figure 11 Predicted and Analytical ( Solid Line ---) Temperature Response for Various Heat Losses and no Control Volume Work.

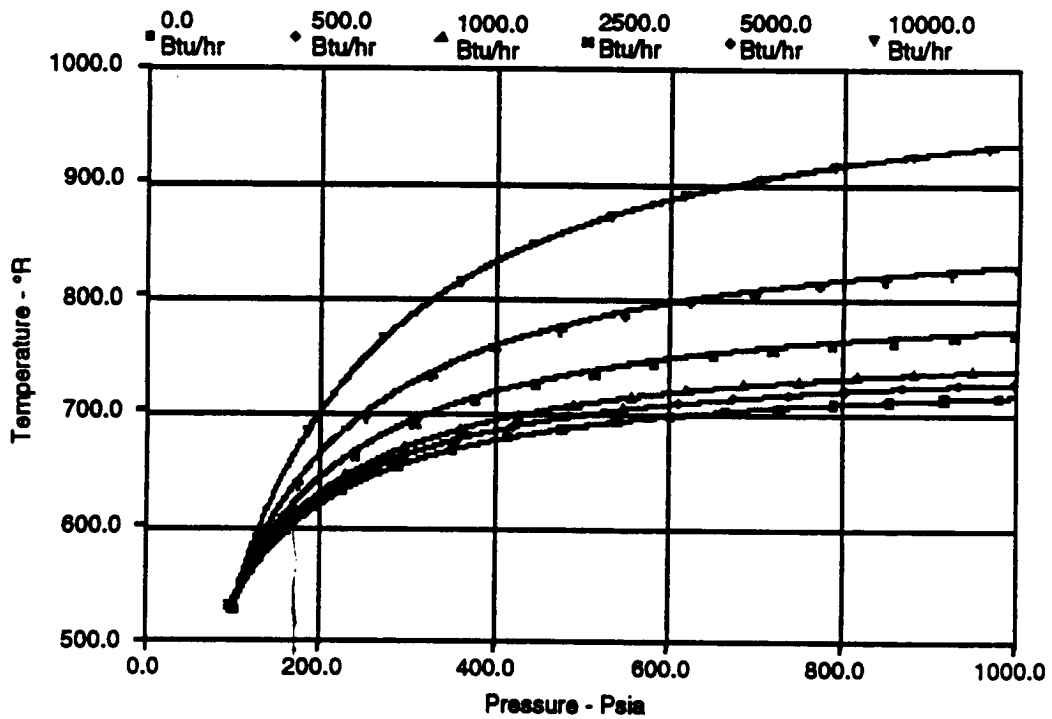


Figure 12 Predicted and Analytical ( Solid Line ---) Temperature Response for Various Heating Rates and no Control Volume Work.

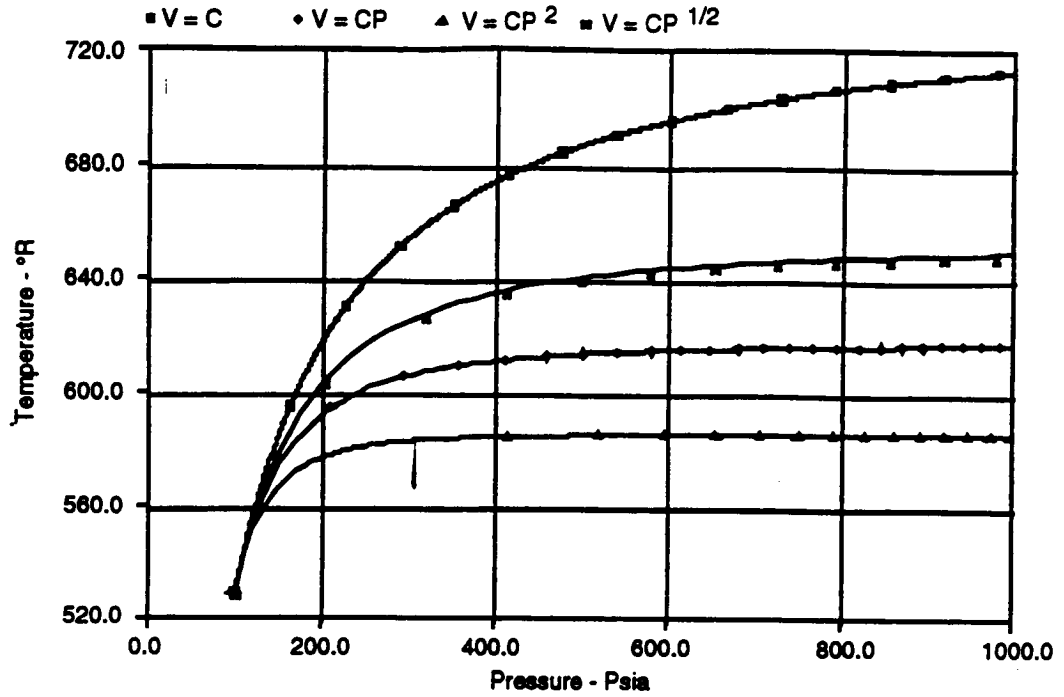


Figure 13 Predicted and Analytical ( Solid Line ----) Temperature Response for Various Pressure-Volume Relationships and no Heat Transfer.

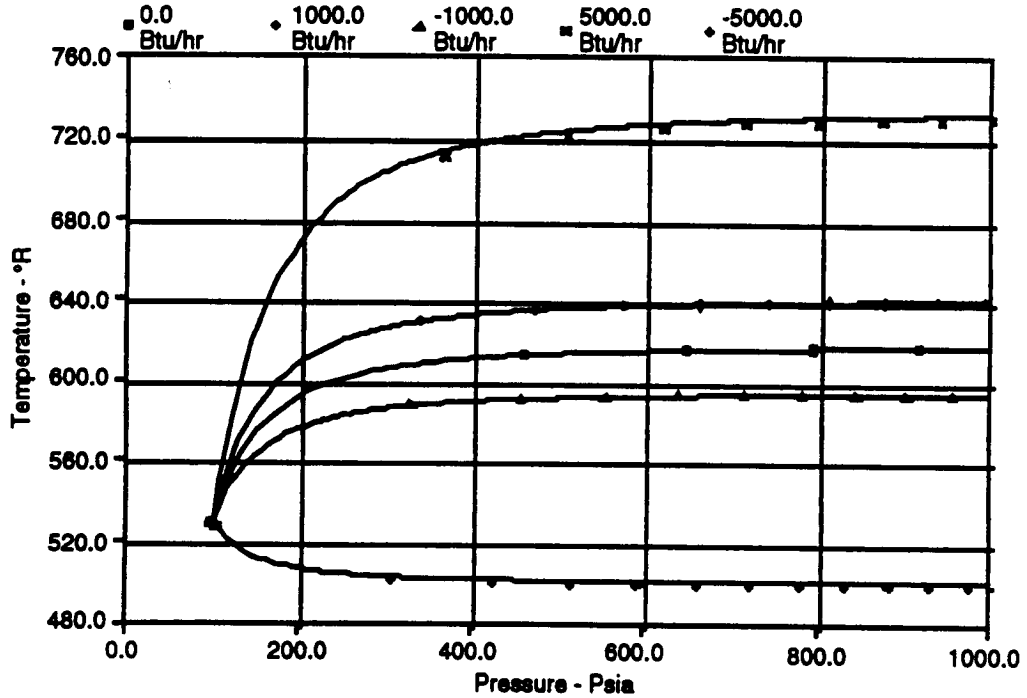


Figure 14 Predicted and Analytical ( Solid Line ----) Temperature Response for Various Pressure-Volume Relationships and Heat Transfer.

## REFERENCES

- 1) Andish, K.K., "SINDA85/FLUINT of the Boeing Thermal Bus System," LESC - 26930, CTSD - 0246, April 1989.
- 2) Keller, J.R., "Revised Predictions of Space Station Airlock Filling Using Updated SINDA85/FLUINT Models," LESC - 28137, March 1990.
- 3) Keller, J.R., "Conversion of the Space Shuttle Active Thermal Control System Models from SINDA/SINFLO to SINDA85/FLUINT," LESC - 27826, CTSD - 0504, December 1990.
- 4) Galate, J.W., Purvis, K.L., and Keller, J.R., "Lunar Transport Vehicle Hangar Thermal Environment Database," LMSC - 2EVA - EV - 078, October 1990.
- 5) De Vahl Davis, G., "Natural Convection of Air in a Square Cavity: A Bench Mark Numerical Solution," International Journal of Numerical Methods in Fluids, Vol 3., pp. 249-261, 1983.
- 6) Chapman, K.S., Johnson J.H., and Chiang, E.C., "The Enhancement and Validation of a Vehicle Engine Cooling Simulation for a Heavy Duty Diesel Truck," SAE Paper #88601, 1988.
- 7) Patanker, S.V., Numerical Heat Transfer and Fluid Flow, Hemisphere, Washington D.C., 1980.
- 8) Harris, R.S., "Verification of the SINDA85/FLUINT Program for Conduction Analysis," LESC - 28200, CTSD - 0614, March 1990
- 9) Keller, J.R., "WP II EVAS Hyperbaric Pressure Control - Final Report," LESC - 27928, January 1990.
- 10) Cullimore, B.A., "Applications of a General Thermal/Hydraulic Simulation Tool," AIAA paper, 1989.
- 11) Iovine, J.V., "SINDA85/FLUINT Benchmark Verification of Single Phase Fluid Flow in a Radiator System," LESC - 28156, March 1990.
- 12) Arpaci, V.S., Conduction Heat Transfer, Addison Wesley Publishing Co., Reading Massachusetts, 1966.
- 13) White, F.M., Fluid Mechanics, McGraw-Hill Book Company, New York, 1979.
- 14) Van Wylen, G.J., and Sonntag, R.E., Fundamentals of Classical Thermodynamics, 3<sup>rd</sup> Edition, John and Sons, New York, 1986.